IISc THESES ABSTRACTS

Thesis Abstract (Ph.D.)

Physical studies on aqueous solutions of mono-substituted ammonium com pounds by R. Bhanumathi.
Research supervisor: S. K. Vijayalakshamma.
Department: Inorganic and Physical Chemistry

1. Introduction

Organic solutes interact with water mainly in two ways. They may be hydrophobic or hydrophilic. Hydrophobic interaction has been generally seen to be enhancing water structure. It has generally been taken to be due to the enhanced hydrogen bonding. Water molecules next to the hydrophobic solute not having any direct interaction in one of the directions, the hydrogen bonds in the other directions are assumed to be strengthened and hence the enhanced structure in hydrophobic solutions. Hydrophilic groups favourably interact with water and form hydrogen bonds. This may give rise to direct and strong interaction of the solute with a limited number of water molecules and these first layer-water molecules participating with the three-dimensional network of hydrogen bonds in water result in an enhanced water structure as compared to solvent water. It is also possible in some cases where the first layer of water molecules are geometrically so situated that they can not participate in the three-dimensional water structure without breaking some hydrogen bonds that are existing in solvent water. In such cases there is a region where the three-dimensional bonds are broken. The overall effect of greater hydrogen bonds in the first layer and a large number of hydrogen bonds broken in the subsequent layers may be a structure less than in the solvent water. These solutes are structure-breaking solutes. In the extreme case, the solute interacts with water but this interaction is not strong enough to form a definite hydrogen bond, but this breaks down the three-dimensional network. These solutes would be strongly structure breaking in nature[1,2].

Alkanes and alkyl groups are hydrophobic in nature. Hydroxyl groups and amino groups are hydrophilic in nature. It is of interest to study the nature of interactions with solute molecules having different types of groups. In the present case, interactions of ammonium chlorides with different substituent groups with water are studied. The compounds taken up for study are – methylammonium chloride, ethylammonium chloride, propylammonium chloride, iso-propylammonium chloride, tert-butylammonium chloride, benzylammonium chloride, ethanolammonium chloride, β-amino ethylene-ammonium chloride, hydroxylammonium chloride and glycine.

2. Experimental

The methods of study used for this work are 1) density measurements, 2) viscosity measurements 3) NMR chemical shift measurements and NMR relaxation time measurements.

2.1 Density measurements[3]

Apparent molal volumes are computed from density measurements of dilute solutions ($c < 0.10$ molar). These are corrected for the contribution of the interionic interaction and the corrected volumes are extrapolated to zero concentration to give partial molal volume.

The partial molal volume of the salt is separated to ionic contributions. Using Teresawa's model, the solute-solvent interaction volume for the individual cations are calculated. The interaction volume is negative in every case, the extent depending on the extent of interaction. This decrement in volume is minimum for the hydrophobic ions and very high for structure-breaking hydrophilic ions.

Making use of Edwards model for solute volume in a solution, the effective hydration number of individual ions is calculated and this is found to vary from a minimum of 2.6 for tert.butylammonium ion to a maximum of 7.5 for glycine and benzyl ammonium ions. This can be taken to represent statistically the number of water molecules in the close vicinity of the solute in solution.

2.2. Viscosity measurements[4]

Viscosity studies have been used for nearly 50 years to examine the type of solute solvents interaction but the results have been mostly qualitative in nature. Making use of Eyring's rate equation and Früth's model for viscous flow, the experimental data on viscosity have been shown to yield the value of surface tension of water in the first layer around the solute molecule[5, 6]. A value of surface tension higher than that of pure water at the same temperature shows unequivocally the solute to be enhancing water structure and a lower value indicates the solute to be structure breaker. The numerical value of the surface tension of the first layer can thus be taken as a quantitative measure of the effect of solute on the water structure.

In the present study of a series of primary ammonium compound, it was found that tert.butylammonium ion ($\gamma = 86$), isopropylammonium ion ($\gamma = 85$), n-propylammonium ion ($\gamma = 74$) and hydroxylammonium ion ($\gamma = 73$) enhance the water structure ($\gamma = 72$); ethylammonium ion ($\gamma = 69$), benzylammonium ion ($\gamma = 62$), ethanol ammonium ion ($\gamma = 61$) and methylammonium ion ($\gamma = 57$), glycine ($\gamma = 43$) and β-amino ethyl-ammonium ion ($\gamma = 39$) breakdown the structure of water.

2.3. NMR chemical shift measurements[7]

NMR chemical shift of water protons of the solvent is found to shift in presence of solute. This shift is found to vary linearly with solute concentration over a range of concentration. The shift of the solvent chemical shift in 1 molar solution is designated as molar chemical shift (δ molar). This molar chemical shift may be downfield (where more hydrogen bonds are present than in pure water) or upfield shift (where some of the hydrogen bonds present in solvent water are broken in presence of solute). The magnitude of the shift and its direction can throw light on the effect of solute on the water structure.

The hydrophilic structure forming solute-like hydroxylammonium chloride gives a downfield molar chemical shift indicating that there are more hydrogen bonds in this solution than in solvent water. Structure-breaking ions like ethanolammonium ion, benzylammonium ion and glycine give an upfield shift indicating that some hydrogen bonds are broken in these solutions. Methylammonium, ethylammonium and propylammonium ions show negligible shift indicating

that on the whole the average of the fraction of hydrogen bonds remain nearly same as in pure water. But strongly structure-forming hydrophobic ions like iso-propylammonium ion and tert.butylammonium ions show an upfield shift. It is generally assumed that the increase in structure in hydrophobic solutions is due to increase in hydrogen bonds. If this were the case, the molar chemical shift would be downfield. In fact this has been found to be the case at low temperatures. But at ambient temperature, the shift is upfield indicating more hydrogen bonds breaking. At ambient temperatures where extensive hydrogen bonds in water are breaking up, it appears that the monomolecular water aligns itself around the hydrophobic solute and thus give rise to upfield shift.

2.4. NMR relaxation times[8]

a) Relaxation times of protons of solvent water

Longitudinal relaxation times (T_1) of solvent protons are measured in aqueous solutions.

Intramolecular relaxation rate $(1/T_1)$ is known to be the sum of two components — intramolecular relaxation rate $(1/T_1)_{intra}$ and intermolecular relaxation rate $(1/T_1)_{inter}$. Intramolecular relaxation rate is separated from the total relaxation rate and rotational correlation times (τ_c) is calculated in each of the cases.

It is found from the results that τ_c of the solvent in ethylammonium chloride solution is comparable with τ_c^c of pure water and this separates the structure-breaking methylammonium chloride from the structure-forming higher homologues. Benzylammonium chloride shows lesser tendency for structure enhancement when compared with alkylammonium chlorides. Glycine has a τ_c which is much less than that of pure water indicating that water in this solution is more free and the structure of water is much less in this case. The τ_c of ethanolammonium chloride and hydroxylammonium chloride solutions are nearly equal to that of pure water.

b) Relaxation times of deuterons of solvent D_2O

Unlike the relaxation time of protons of solvent water, the relaxation time of deuterons of solvent deuterium oxide is directly related to the correlation time of D_2O molecule. In this case the relaxation mechanism is mostly by the quadrupolar coupling of the deuterium nucleus and this falls off very rapidly with distance. So the contributions to the relaxation is mainly from the intramolecular mechanism.

In the present series of salts, the deuterium relaxation rate of solvent D_2O has been experimentally determined and correlation times calculated. This shows a gradual increase in the structure-forming tendency with chain length or bulk of alkyl groups. Introduction of polar groups like –OH as in the case of ethanolammonium chloride reduces the structure-forming tendency. Introduction of phenyl group as in benzylammonium chloride increases the structure of water because of the interaction of π electron cloud with water. Correlation time of water in the close vicinity of the cations has been calculated using the model of hydration of Hertz *et al.*

3. Conclusions

Examination of the systems from different angles using different methods has given a clearer picture of the solute-solvent interaction in these cases. Around solutes like tert.butylammonium chloride, iso-propylammonium chloride and n-propylammonium chloride exist cage-like structures

of water in aqueous solution. The water is bound more strongly than in water but this bonding is not due to the usual hydrogen bonds. Hydroxylammonium chloride is hydrogen bonded to the solvent water and there is an enhanced water structure in the immediate vicinity of this salt. But there is a structure broken region beyond the first layer which is responsible for lower correlation time of solvent water in these solutions. Though ethanolammonium chloride forms hydrogen bonds with water, this salt does not increase the structure of water even in the close vicinity. β-amino ethylammonium chloride and glycine positively break down the water structure. Benzylammonium chloride also breaks down the water structure but this interacts favourably with water molecules because of the π electrons of the aromatic ring. This is clearly seen in the enhanced correlation times of water in benzylammonium ion solutions.

References

1. CONWAY, B.E.   *Ionic hydration in chemistry and biophysics*, Elsevier, Amsterdam, 1981.

2. FRANKS, F. (Ed.)   *Water—a comprehensive treatise*, Vols. 2 and 3, Plenum Press, New York, 1973.

3. MILLERO, F.J.   *Chem. Rev.*, 1971, **71**, 147.

4. STOKES, R.H. AND   *Viscosity of electrolytes and related properties*, Pergamon Press, 1965.
   MILLS, R.

5. FEAKINS, D.   *J. Chem. Soc. Faraday Trans.* I, 1974, **20**, 795.
   FREEMANTLE, D. AND
   LAWRENCE, K.G.

6. GOLDSACK, D.E. AND   *Can. J. Chem.*, 1978, **56**, 1442.
   FRANCHETTO, R.C.

7. DAVIES, J.   *J. Chem. Soc. Faraday Trans. II*, 1972, **68**, 686.
   ORMONDROYD, S. AND
   SYMENS, M.C.R.

8. GOLDAMMER E.V.   In *Modern aspects of electrochemistry*, No. 10, J. O. M. Bockris and B.E. Conway (Ed.), Plenum Press, New York, 1978, 1.

Thesis Abstract (Ph.D.)

Studies of phosphazenes: (i) Synthetic and kinetic investigations on the reactions of hexachlorocyclotriphosphazene with aromatic primary amines and (ii) Synthesis and reactivity of poly(dichlorophosphazene) by S. Ganapathiappan.
Research supervisors: S. S. Krishnamurthy and A. R. Vasudeva Murthy.
Department: Inorganic and Physical Chemistry.

1. Introduction

The main objective of this work is to synthesize phosphazene-based polymers which may find applications at both low and high temperatures. Two methods have been utilized for the synthesis of phosphazene-based polymers. The first one involves condensation polymerization of hexachlorocyclotriphosphazene ($N_3P_3Cl_6$) with aromatic diamines. Several difficulties are encountered in characterizing the products formed in the above reactions. In order to assess the

reactivities of these diamines towards $N_3P_3Cl_6$, kinetic studies of the first and second stages of chlorine replacement from $N_3P_3Cl_6$ by aromatic primary amines -- aniline, p-toluidine and p-anisidine -- have been investigated as "model systems"[1,2].

2. Synthetic and spectroscopic studies

Detailed synthetic studies have been carried out under a variety of experimental conditions to ascertain the nature of products formed in these reactions. The cyclophosphazene derivatives, $N_3P_3Cl_{6-n}$ $(NHC_6H_4R-p)_n$ [R = H, Me or OMe, n = 1, 2(three isomers); R = OMe, n = 3(three isomers); 4(geminal isomer only), 5 and 6] have been isolated and characterized. At the second stage of chlorine replacement, nongeminal derivatives are formed predominantly when diethyl ether, THF or methyl cyanide is used as the reaction medium; however, in the presence of triethylamine, geminal derivative is formed exclusively. The structures of the cyclophosphazene derivatives isolated have been determined on the basis of ^{31}P NMR spectroscopy. Isomeric compositions for the nongeminal derivatives are deduced from the ^1H NMR spectra of the corresponding dimethylamino and/or methoxy derivatives[3].

3. Kinetic studies

Kinetic studies reveal that the first and second stages of chlorine replacement in THF and methyl cyanide occur by a $S_N2(P)$ mechanism. Rate constants and activation parameters have been evaluated. The associative $S_N2(P)$ mechanism may involve either the formation of a penta-coordinated intermediate or a concerted pathway without the intervention of such an intermediate. Evidence for both types of mechanisms are obtained. Kinetic studies also reveal that the second stage of chlorine replacement in THF in the presence of an excess of tri-n-butylamine occurs by a base-catalysed E_1 CB mechanism which involves the formation of a tricoordinate pentavalent phosphorus intermediate. The formation of such an intermediate is conclusively established by trapping experiments with methanol and by the isolation of the unusual products, gem-$[N_3P_3Cl_4 (NHC_6H_4R-p) (O)]^-$ $(NHEt_3)^+$ (R = H, Me or OMe)[4].

4. Phosphazene polymers

The second approach investigated for the synthesis of P-N polymers involves the ring-opening thermal polymerization of $N_3P_3Cl_6$ at 250°C and the subsequent replacement of chlorine atoms from the linear poly(dichlorophosphazene), $[NPCl_2]_n$ by a variety of organic groups. The effect of various compounds viz., triphenylphosphine, benzoic acid, $N_3P_3Cl_6$ $(NPPh_3)$, $N_3P_3Cl_3$ $(NMe_2)_3$ and $CaSO_4 \cdot 2H_2O$ as initiators for the thermal polymerization of $N_3P_3Cl_6$ has been investigated. Among the various compounds studied, $CaSO_4 \cdot 2H_2O$ has proved most effective for the synthesis of $[NPCl_2]_n$ with a high molecular weight ($> 5 \times 10^6$) in 60% yield. The rationale for the choice of the catalysts and the mechanism of polymerization of $N_3P_3Cl_6$ in the presence of the above initiators are discussed. Several homo-polymers and mixed substituent polymers of the following compositions, $[NP(OPh)_x(OR)_{2-x}]_n$ (R = C_6H_4Me-p, CH_2CF_3 or $CH_2CH = CH_2$; x = 0 -- 2) have been prepared and characterized. The thermal properties of these polymers are also discussed[5].

References

1. KRISHNAMURTHY, S.S.,   Adv. Inorg. Radiochem., 1978, 21, 41.
   SAU, A.C. AND
   WOODS, M.

2. ALLCOCK, H.R.   Chem. Engng. News, 1985, **63**, 22.

3. GANAPATHIAPPAN, S. AND   J. Chem. Soc., Dalton Trans., 1987, 579.
   KRISHNAMURTHY, S.S.

4. GANAPATHIAPPAN, S. AND   J. Chem. Soc., Dalton Trans., 1987, 585.
   KRISHNAMURTHY, S.S.

5. GANAPATHIAPPAN, S.,   Macromolecules, 1987, **20**, 1501.
   DHATHATHREYAN, K.S. AND
   KRISHNAMURTHY, S.S.

Thesis Abstract (Ph.D.)

Thermal expansion studies on irradiated polymers at low temperatures by H. N. Subrahmanyam.

Research supervisor: S. V. Subramanyam.
Department: Physics.

1. Introduction

The study of thermal properties of irradiated polymers at low temperatures is significant both from the scientific and technological point of view. Irradiation offers a powerful tool to polymer physicist to modify the structure of polymers and to study the effects of these modifications on the properties of polymers. The increasing use of various polymers at low temperatures and radiation environments confers a special technological importance to such a study. When compared to the study of mechanical and electrical properties, the study of thermal properties of irradiated polymers have attracted very little attention. Even among the thermal properties, while there are a few investigations on specific heat and thermal conductivity, no study has been reported on thermal expansion. This thesis reports the thermal expansion at low temperatures (80 to 340 K) of four commercial polymers – Polymethyl methacrylate (PMMA), Polystyrene (PS), Polytetrafluoroethylene (PTFE), and Polyoxymethylene (POM) – irradiated by using gamma radiation from Co^{60} source.

After a brief introduction to theoretical understanding of thermal expansion of solids, a brief review of different aspects of thermal expansion of polymers is given. This includes the discussion of thermal expansion of polymer crystals, thermal expansion of oriented polymers, the effect of crystallinity changes on thermal expansion, thermal expansion behaviour during relaxational transitions in polymers and the Gruneisen parameters of polymers. A brief review of the different experimental techniques employed for accurate measurement of thermal expansion at low temperatures, with a special emphasis on the three terminal capacitance technique which is employed in the present investigation, is also given. A few important effects of irradiation on polymers, pertinent to the present work, are discussed.

2. Experimental details

The design and fabrication of a capacitance cell and a cryostat for use in the thermal expansion experiments in the temperature range 80 to 340 K is described[1]. Capacitance is measured by using a six decade ratio transformer with a resolution of 1 part per million. This gives a resolution better than an angstrom in the change in length of a sample of length 1 cm. The temperature of

the sample is measured by a platinum resistance thermometer to a resolution of 0.1 K. The capacitance cell, being a differential one, is calibrated by using high purity aluminium and germanium as standard reference materials. The experimental data is analysed by using a cubic spline computer program. The accuracy in the thermal expansion measurement is 4%.

The polymer samples are irradiated in air to various integral dosages by using gamma radiation from a Co^{60} source at room temperature. The IR spectra of all the samples are recorded to codify the radiation-induced changes. The changes in crystallinity of the semicrystalline polymers (PTFE & POM) are measured by x-ray technique. The crystallinity is found to increase in both these samples.

2.1 PMMA

The thermal expansion coefficient of PMMA is found to increase with irradiation, the increase being larger at higher temperatures. This is due to the relative increase in Van der Waals bonding resulting from the main chain scission by irradiation[2].

2.2 Polystyrene

In PS, the thermal expansion coefficient is found to decrease at low temperatures while it increases at high temperatures due to irradiation. PS undergoes simultaneous crosslinking and degradation on irradiation in air. The decrease in thermal expansion coefficient at low temperatures is due to crosslinking whereas the increase at high temperatures is due to degradation[3].

2.3 PTFE

The thermal expansion coefficient of PTFE is found to increase with radiation dose below its glass transition temperature while above this temperature it decreases. The increase below glass transition temperature is due to degradation and the decrease above this temperature is due to enhanced crystallinity. The two first-order phase transitions are found to shift to lower temperatures due to degradation[4].

2.4 Polyoxymethylene

In the case of POM, the thermal expansion coefficient increases with radiation dose below and decreases with radiation dose above the glass transition temperature. The predominant effect of degradation below the glass transition and that of increased crystallinity above the glass transition are responsible for this behaviour[5].

References

1. SUBRAHMANYAM, H.N. AND SUBRAMANYAM, S.V.
Accurate measurement of thermal expansion of solids between 77 K and 350 K by 3 terminal capacitance method, *Pramana*, 1987, **27**, 647–660.

2. SUBRAHMANYAM, H.N. AND SUBRAMANYAM, S.V.
Thermal expansion of irradiated polymethylmethacrylate, *Polymer*, 1987, (under publication).

3. SUBRAHMANYAM, H.N. AND SUBRAMANYAM, S.V.
Thermal expansion of irradiated polystyrene, *J. Mater. Sci.*, 1987, **22**, 2079–2082.

4 SUBRAHMANYAM, H.N. AND   Thermal expansion of irradiated polytetrafluoroethylene, *J Polym. Sci.,*
   SUBRAMANYAM, S.V.   *Part II Polymer Physics*, 1987, **25** (under publication).

5 SUBRAHMANYAM, H.N. AND   Thermal expansion of irradiated polyoxymethylene, *Eur Poly. J.,* 1987, **23,**
   SUBRAMANYAM, S.V.   207–211.

Thesis Abstract (Ph.D.)

Strength and behaviour of reinforced concrete wall panels by S. Madina Saheb.
Research supervisor: Prakash Desayi.
Department: Civil Engineering.

1. Introduction

Reinforced concrete load bearing wall panels, hitherto, are being analysed and designed on the analogy of extended columns in one-way action only irrespective of their end conditions. But a wall panel in practical situation could behave like a plate in two-way action when all the four edges are restrained. Also in these panels large openings in the form of doors and windows are inevitable due to functional requirements. In all the above cases, information regarding the strength and behaviour of panels as influenced by geometry, materials of construction, end conditions and type of loading is required for developing design methods based on limit concepts. The available information on panels in one-way action is not complete with respect to all parameters, particularly the aspect ratio, while no method or equation for prediction of ultimate strength of panels in two-way action under eccentric loading and panels with openings has been come across in literature.

2. Experimental programme

The present theoretical and experimental investigations carried out have been intended to lead to some methods of predicting ultimate strength and an insight into the behaviour of a) panels in one-way action; b) panels in two-way action; and c) panels with openings, and subjected to uniformly distributed load at small eccentricity of one-sixth the wall thickness. The ends of panels are idealized to be hinged so that the test data would be conservative for development of design equations. The panel reinforcement is selected to be in double layers for effective load resistance under eccentricity and protection against temperature and shrinkage effects.

For the said investigation, aspect ratio, slenderness ratio, thinness ratio, amount of vertical steel, amount of horizontal steel, size and location of openings in panels have been identified as pertinent parameters. To cover all the parameters, a total of 60 panels were cast and tested. In all the three aspects of study, strains, deflections, cracking loads and failure loads have been recorded and presented.

3. Main results and conclusions

(i) Panels in one-way action

The influence of aspect ratio and vertical steel on ultimate strength are linear while that of slenderness ratio is nonlinear. The effect of horizontal steel on ultimate strength is negligible. An empirical equation which includes the effect of aspect ratio also for the prediction of ultimate strength (P_u) has been developed as given below.

$$P_u = 0.55\phi\left[Af'_c + (f_y - f'_c)A_s\right]\left[1 - \left(\frac{h}{32t}\right)^2\right]\left[1.20 - \frac{h}{10L}\right]$$

for $h/L < 2.0$ (1a)

and $P_u = 0.55\phi\left[Af'_c + (f_y - f'_c)A_s\right]\left[1 - \left(\frac{h}{32t}\right)^2\right]$

for $h/L \geq 2.0$ (1b)

where ϕ = capacity reduction factor
      A = gross cross-sectional area of wall panel in plan
      A_s = cross-sectional area of steel in panel
      f'_c = cylinder strength of concrete
      f_y = yield stress of steel
      h = height of wall panel, and
      L = length of wall panel.

Figure 1 shows the comparison of test results of the author and other investigators[1-4] with proposed equation for $\phi = 1.0$. Also, on comparison with available wall equations in literature, the proposed equation is noted to give safer prediction of ultimate strength. Three methods of analysis *viz.*, moment maximization, additional moment and moment magnification have been proposed for prediction of ultimate strength of panels. It is concluded that the moment magnification method gives satisfactory prediction of ultimate strength when compared with the other two. The three different code methods of analysis namely ACI: 318–77, CP: 110–72 and IS: 456–78 have also been compared with test results and it is found that the ACI: 318–77 method gives a better prediction of ultimate strength while the other two are more conservative.

(ii) Panels in two-way action

The influence of aspect ratio and vertical steel on ultimate strength are linear while that of thinness ratio is non-linear. The effect of horizontal steel on ultimate strength is fairly linear for panels with aspect ratio greater than unity. Two empirical equations, one based on safe prediction principle and the other by modification of ultimate strength equation of a thin buckled metal plate, have been proposed as given below:

Wall equation I,

$$P_u = 0.37\phi f'_c A\left[1 - \left(\frac{L}{120t}\right)^2\right]\left[1 + 0.12\frac{h}{L}\right]$$

for $2 > h/L > 0.5$ and $L/t < 60$.   (2)

Wall equation II,

$$P_u = \frac{C\phi Af'_c}{(L/t)}$$ (3)

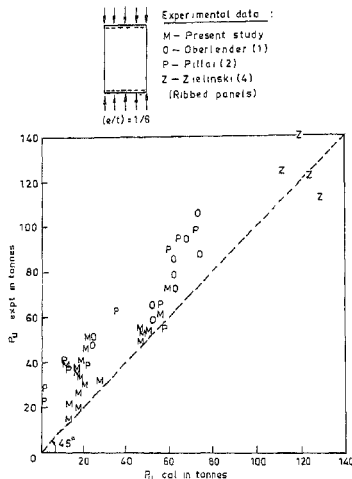where C = plate constant = $0.8352\,L/t - 0.0052\,(L/t)^2$

for $L/t < 60$.

FIG. 1 Comparison of test results with proposed
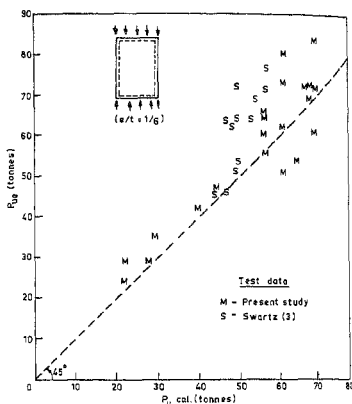equation (one-way action for $\phi = 1.0$).

FIG. 2 Comparison of test results with proposed
equation – I (two-way action for $\phi = 1.0$).

Figure 2 shows the comparison of test results of the author and another investigator[3] with
proposed wall equation I (eqn 2). It is found that both the equations give satisfactory prediction of
ultimate strength.

The solution of the problem for panels in two-way action under eccentric loading has been
attempted by a semi-theoretical method based on moment magnification principle. The proposed
method is noticed to yield ultimate strengths fairly in agreement with test data for aspect ratios
up to 1.5. From the comparative study made for strength and behaviour between panels in
one-way and two-way actions, it is concluded that the load resistance and stiffness of panels in
two-way action are greater than those in one-way action.

(iii) Panels with openings

To study the effect of size and location of openings on ultimate strength and behaviour of panels,
a non-dimensional parameter (ν) has been defined in the investigation as given below:

$$\nu = \left(\frac{A_0}{A} + \frac{\eta}{L}\right) \tag{4}$$

where, A_0 = cross sectional area of opening in plan, and
η = distance between centres of gravity of panel cross-section with and without
openings.

The influence of this parameter on ultimate strength is found to be linear within the tested range
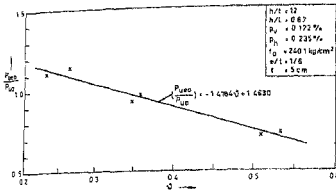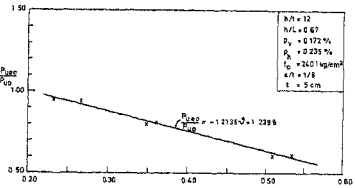
Fig. 3 Effect of openings (one-way action).   Fig. 4 Effect of openings (two-way action).

of variables. Figures 3 and 4 show the influence of openings in panels in one-way and two-way actions respectively.

Empirical equation developed for the prediction of ultimate strength of panels both in one-way and two-way actions are (figs 3 and 4):

$$\frac{P_{ueo}}{P_{uD}} = -1.4184\nu + 1.4630 \qquad (5)$$

(one-way action)

$$\frac{P_{ueo}}{P_{uD}} = -1.2136\nu + 1.2398 \qquad (6)$$

(two-way action)

where P_{ueo} = ultimate experimental load of panel with openings, and
P_{uD} = ultimate theoretical load of panel without openings.

These equations are found to give satisfactory prediction of ultimate strength. A comparative study of the strength and behaviour between panels with openings in one-way and two-way actions has been made and it is concluded that the load resistance and stiffness of panels in two-way action are greater than those in one-way action in the presence of openings also.

In all the three aspects of study, the results obtained are expected to be useful in the development of limit state design procedures of such panels. The empirical equations proposed for the prediction of ultimate strength of panels for different cases are in a form which can be directly introduced into codes of practice.

References

1. OBERLENDER, G.D.   *Strength investigation of precast reinforced concrete load bearing wall panels,* Ph.D. dissertation, University of Texas, Arlington, 1973.

2. PILLAI, S.U. AND PARTHSARATHY, C.V.   Ultimate strength and design of concrete walls, *Bld Environment,* 1977, **12,** 25–29.

3. SWARTZ, S.E., ROSE BRAUGH, V.H. AND BERMAN, M.Y.   Buckling tests on rectangular concrete panels. *JACI,* 1974, **71,** 33–39.

4. ZIELINSKI, Z.A., TROITSKY, M.S. AND CHRISTODOULOU, H.   Full scale bearing strength investigation of thin wall-ribbed reinforced concrete panels, *JACI,* 1982, **79,** 313–321.

Thesis Abstract (Ph.D.)

Studies on drop formation at conical and capillary tips by S. Ramesh Babu.
Research supervisors: A. K. Lahiri and M. Mohan Rao.
Department: Metallurgy.

1. Introduction

Despite the role of drops being recognised in many metallurgical processes, surprisingly no
significant progress has been made in this area. An understanding of the drop formation
phenomenon is expected to give a better insight of the associated mass transfer and heat
transfer aspects of the relevant processes. Keeping this in view, the present studies on drop
formation at conical tips, which is a first step towards a better understanding of drop formation at
the tips of the melting rods, of direct relevance in a metallurgical process such as ESR, were
taken up. The studies on drop formation at capillary tips provided a useful analogy for those at
conical tips. Both theoretical and experimental approaches have been employed for the analysis
of drop formation.

2. Theoretical analysis

The principle of minimisation of free energy has been used to develop a mathematical model to
predict the equilibrium profiles of pendent drops forming at infinitely slow rates at conical tips,
using the variational approach[1]. The same governing equations have been shown to be deducible
by an alternate approach using the force balance criterion. The dimensionless profile generating
equations were solved using fourth order Runge-Kutta method for which a computer programme
was developed ensuring an accuracy of better than one part per million in the computed values.
The model permits the calculation of drop volume as well as to follow the changing sequence of
drop profiles until the onset of instability. The maximum drop volume is shown to increase with
cone angle. Also, it is shown through the model that for a specified cone angle there is a critical
rod diameter beyond which the maximum drop volume forming at its conical tip is independent of
the rod diameter. Drop formation at conical tips with base diameter less than the critical diameter,
referred to as finite cones has also been analysed until the onset of instability and the effect of
rod diameter, cone angle and physical properties of the system on the shape and maximum drop
volume are predicted. An absolute method for the determination of surface tension of liquids
using the pendent drop profiles at conical tips, which is shown to be superior to other pendent
drop profile methods, has been proposed.

A special case of the model is the analysis of drop formation at a flat surface. A notable feature
of this is the possibility of multiple drop formation when the cross-sectional area of the flat
surface is considerably greater than the critical contact area of the drop. As a result of the
enhanced drop-continuous phase reacting interface, multiple drop formation can be utilized in
processes where refining is of paramount importance.

Using suitable boundary conditions, the present model can also describe the drop formation at
capillary tips which has been extensively studied for well over a century, especially by chemical
engineers. By deducing a force balance criterion from the profile generating equations, it has
been shown that, in general, the Harkins-Brown's[2] empirical correction factors proposed in 1919,
in connection with the determination of surface tension of liquids by drop-weight method, do not

represent the true fractional detachment of drops. Instead, modified correction factors have been proposed. Utilizing these factors, in conjunction with the extension of the similarity criterion proposed by Worthington, a semi-empirical model has been proposed for predicting the detached drop volumes at conical tips.

The model for describing the drop formation at capillary tips has been extended for finite flow rate conditions as well. The numerical results show that the equilibrium drop volume and profile are insensitive to fluid flow rate over a very wide range. Also, based on this model, a criterion for the onset of jetting has been proposed. Semi-empirical models have also been proposed for the prediction of detached drop volumes at capillary tips under finite flow rate conditions. The finite flow rate model is shown to reduce to the infinitely slow flow rate model, when the flow rate tends to zero. The drop formation at conical tips under finite flow rate conditions is analysed using a dimensional analysis approach and a correlation between the detached drop volume and flow rate has been obtained.

Also, Harkins-Brown's most reliable drop weight data at capillary tips, has been statistically analysed and utilizing the mathematical description of the relation between dimensionless detached drop volume and the dimensionless capillary radius, two alternate methods have been proposed for the calculation of surface tension of liquids. Using the error analysis approach, the proposed methods have been shown to be better than the earlier methods[3] over a wide operating range.

3. Experimental results and discussion

A set of apparatus has been designed and fabricated for studies on drops forming at metal cone tips of specific cone angle under controlled flow rates, for quantitative verification of the predictions of the model. Using these apparatus, experiments have been performed with low vapour pressure liquids 1,1,2,2-tetrachloroethane and chlorobenzene, to study the effect of cone angle, rod diameter, flow rate and physical properties of the liquids on drop size. The trends in the theoretical predictions mentioned earlier have been shown to be in very good agreement with the experimental results. The drop formation phenomenon was followed through movie-photography and the agreement between the drop profiles and the maximum drop volumes with the theoretical predictions have been shown to be excellent. However, the predicted detached drop volumes are shown to be underestimated, with a maximum percentage deviation of 27%. The reasons for the discrepancy have been discussed. The analysis of the cine films have also yielded useful information on the mechanism of detachment and the instability time has been estimated for each of the conical tips of 60, 90, 120, 150 and 180°, studied. The dimensionless detached drop volumes at each of the conical tips for both the liquids studied have been shown to be identical, which supports the assumption behind the extended Worthington's similarity criterion. Also, this forms the basis of a comparative method for the determination of surface tension of liquids.

Experiments have been performed at a capillary tip to study the effect of flow rate on drop formation. The experimentally obtained critical profile and the equilibrium drop volume closely tallies with those predicted theoretically. Also, the detached drop volumes calculated using the proposed models are shown to be in good agreement with the experimental values.

To test the validity of the predictions of the models discussed above in drop formation at the tips of melting rods, which has greater relevance to metallurgists, a low-temperature experimental set-up was designed and fabricated for melting studies using paraffin wax

material – the liquid state transparency of which has enabled photographic recording of the drop formation phenomenon. The experiments consisted of melting the stationary wax rods having conical tips in a hot accetonitrile/alcohol bath and collecting the solidified wax drops below. The effect of rod diameter, cone angle, immersion depth and bath temperature on the drop size was studied. While the trends of the experimental results were in conformity with the theoretical predictions, quantification of the experimental data was not possible owing to uncertainties in the physical properties of the experimental system, despite efforts to minimise these effects.

References

1. RAMESH BABU, S.   J. Colloid Interface Sci., 1987, 116, 350.

2. HARKINS, W. D. AND   J. Am. Chem. Soc., 1919, 41, 499.
   BROWN, F. E.

3. WILKINSON, M. C.   J. Colloid Interface Sci., 1972, 40, 14.

Thesis Abstract (M.Sc. Engng)

Studies on the design and development of a novel fiber optic sensor-based refractometer-cum-liquid level indicator by M. K. Ravishankar.
Research supervisor: S. V. Pappu.
Department: Electrical Communication Engineering.

1. Introduction and experimental programme

Fiber optic sensors (FOS) possess unique advantages over other kinds, and hence a good lot of work is being done in recent years regarding the development of FOS for various applications [1,2]. The measurement of refractive index and detection of liquid levels in a system are important in some industrial applications. Hence, a few fiber optic refractometers and liquid level indicators have been proposed [3-5]. These have a restriction of measurement of refractive index equal to that of the core index, whereas the present liquid level sensors are cumbersome in their design. Hence there exists a need for the design and development of better fiber optic sensors for measuring refractive index of any value and possess easy design criteria for liquid level measurement.

2. Main results and conclusion

The underlying principle of the refractometer and liquid level indicator is that the efficiency of light coupled between two axially separated fibers (fig. 1) varies as a function of the refractive index of the medium filling the axial gap, the refractive index of the core, the axial gap length Z. These parameters are expressed in terms of: (a) Fresnel transmittivity between the end faces of the two fibers which depends on the value n_x and n_c where n_x and n_c represent the refractive index of the
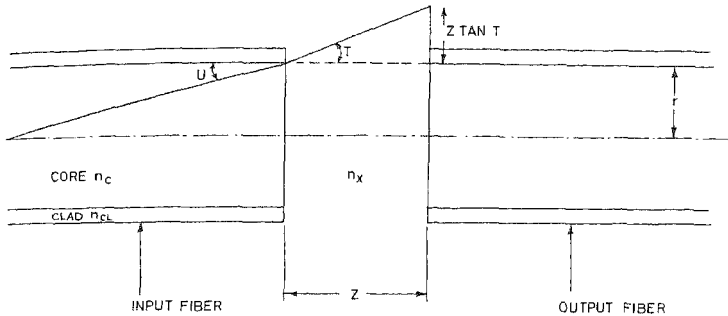
Fig. 1 Schematic diagram of two axially separated optical fibers for illustrating the principle of light coupling between them. U is the angle of incidence, T the angle of emergence, n_c the core refractive index, n_x, the refractive index of the liquid filling the axial gap, r, the core radius, n_{cl} the clad refractive index and Z the axial gap distance.

medium filling the axial separation and that of the core of the fiber[6] (b) The axial gap length 'Z' essentially represents the amount of light energy that can be collected by the output fiber from the input fiber[7]. Thus efficiency of coupling is mathematically given by

$$n = \frac{p_0}{p_i} = F^2 \times \left\{ 1 - \frac{Z}{4r} \tan T \right\} \tag{1}$$

where p_o is the optical power just after the input end of output fiber, and p_i the optical power just before the output end of input fiber:

The upper limit of measurable value of refractive index is fixed by expression (1), whereas the lower limit is fixed by the condition $\tan T \leq r/z$ under which the term

$$\left\{ 1 - \frac{Z}{4r} \tan T \right\}$$

holds valid, where 'r' is the radius of the fiber. The expression exhibits an increase in upper limit, reduction in lower limit and decrease in range of operation coupled with improved sensitivity as the value of Z increases.

The theoretical max value of Z for the fibers used (N.A = 0.5, n_c = 1.49, r = 0.5 mm at λ = 665 nm) is 0.866 mm. The experiment conducted with Z = 0.8 mm using water glycerol mixture for different refractive index values tallied well within 3.6% of the theoretical value for n_x values from 1.33 to 1.52. The change of η for n_x from 1.00 to 1.33 is about n 15.8%, experimentally which has provided enough change in intensity for detection of liquid levels. This involved an input fiber bent to U-shape and the output fiber aligned with it to have an axial gap Z at premarked height to indicate the height of the liquid level.

References

1. GIALLORENZI, T.G.,   Optical fiber sensor technology, *IEEE J. Quant. Electronics*, 1982, QE–18,
   BUCARO, J.A.,   626-665
   DANDRIDGE, A.,
   SIGEL, G.H.JR.,
   COLE, J. H.,
   RASHLEIGH, S.C. AND
   PRIEST, R.G.

2. CULSHAW, B.   *Optical fiber transducers*, Radio Electronic Engr, 1982, **52**, 283-290.

3. TAKEO, T. AND   Optical fiber sensor for measuring refractive index, *Jap. J. Appl. Phys.*,
   HATTORI, H.   1982, **21**, 1509-1512.

4. KUMAR, A.,   Novel refractometer using a tapered optical fiber, *Electronics Letters*, 1984,
   SUBRAHMANYAM, T.V.B.,   **20**, 534-535.
   SHARMA, A.D.,
   THYAGARAJAN, K.,
   PAL, B.P.
   AND GOYAL, I.C.

5. ROSS, I.N. AND   Optical monitoring of glucose concentration, *Opt. Laser Technol.* (UK),
   MBANU, A.   1985, **17**, 31-35.

6. BORN, M. AND   *Principles of optics*, Pergamon Press, New York, 1975, pp. 35–48.
   WOLF, E.

7. YOUNG, M.   Geometrical theory of multimode optical fiber-to-fiber connectors, *Opt.
                               Commun.*, 1973, **7**, 253-255.